

Nitrogen-mediated fabrication of transition metal-carbon nanotube hybrid materials

Seong Ho Yang, Weon Ho Shin, Jung Woo Lee, Hyun Seok Kim, Jeung Ku Kang et al.

Citation: *Appl. Phys. Lett.* **90**, 013103 (2007); doi: 10.1063/1.2428411

View online: <http://dx.doi.org/10.1063/1.2428411>

View Table of Contents: <http://apl.aip.org/resource/1/APPLAB/v90/i1>

Published by the [American Institute of Physics](http://www.aip.org).

Additional information on *Appl. Phys. Lett.*

Journal Homepage: <http://apl.aip.org/>

Journal Information: http://apl.aip.org/about/about_the_journal

Top downloads: http://apl.aip.org/features/most_downloaded

Information for Authors: <http://apl.aip.org/authors>

ADVERTISEMENT



Goodfellow
metals • ceramics • polymers • composites
70,000 products
450 different materials
small quantities fast

www.goodfellowusa.com

Nitrogen-mediated fabrication of transition metal-carbon nanotube hybrid materials

Seong Ho Yang, Weon Ho Shin, Jung Woo Lee, Hyun Seok Kim, and Jeung Ku Kang^{a)}
*Department of Materials Science and Engineering, KAIST, 373-1, Guseong-dong, Yuseong-gu,
 Daejeon 305-701, Republic of Korea*

Yoon Kee Kim
*Department of Materials Science and Engineering, Hanbat National University, Daejeon 305-719,
 Republic of Korea*

(Received 11 September 2006; accepted 29 November 2006; published online 3 January 2007)

The authors report the simple and easy method to fabricate transition-metal-carbon nanotube hybrid materials through nitrogen mediation. Ni nanoparticles were uniformly dispersed on carbon nanotubes without any pretreatment such as defect activation by strong acids or covalent functionalization processes. A theoretical study of the nitrogen-mediated mechanism using first-principles density functional theory calculations is also presented. The first-principles calculations reveal that pyridinelike nitrogen in carbon nanotubes significantly enhances the binding energy of Ni interacting with carbon nanotubes. © 2007 American Institute of Physics.

[DOI: [10.1063/1.2428411](https://doi.org/10.1063/1.2428411)]

Carbon nanotubes (CNTs) interacting with transition metal atoms are of tremendous interest from both fundamental and applied perspectives.¹⁻⁹ Applications reported include hydrogen storage media, sensor materials, nanomagnets, catalysts, and nanoelectronic devices. Kong *et al.*² have shown that excellent molecular hydrogen sensors can be realized by decorating single-walled CNTs with Pd nanoparticles. Kim *et al.*⁴ have reported that Ni nanoparticles on multiwalled CNTs significantly enhance hydrogen storage capacity. It has also been demonstrated that transition metal nanoparticles on CNTs exhibit superior catalyst activities for various types of chemical reactions.¹⁰⁻¹³ In order to establish uniformly dispersed metal nanoparticles on CNT sidewalls, the CNTs need to be functionalized, since they are chemically highly inert. Oxidative damage by strong acids can activate intrinsic defects, which generates oxygenated functional groups.¹⁴⁻¹⁶ Covalent functionalization methodologies using a highly reactive intermediate to attack CNTs have also been developed.¹⁶⁻¹⁹ Unfortunately, many of the thermal, optical, electrical, and mechanical properties of CNTs are dependent on π conjugation. Therefore, functionalization can result in the deterioration of these qualities. Moreover, functionalization procedures often require harsh solvents with extended reaction time to activate the sidewalls of CNTs, which is not desirable from an economical viewpoint.

Generally, the doping of other elements is a practical method of tailoring the electronic properties of materials. Similarly, the substitution of nitrogen for carbon in the graphitic layer of CNTs results in a change in the electronic structure and thus alters the chemical reactivity.²⁰⁻²² Nitrogen doped CNTs contain nitrogen atoms as localized defects that make the sidewalls of CNTs chemically active. Therefore, it is expected that metal-CNT hybrid materials could be fabricated through nitrogen mediation without any functionalization processes. In this letter, we report a simple method to fabricate uniformly dispersed Ni nanoparticles on nitrogen doped multiwalled carbon nanotubes (CN_xMWNTs) without

any functionalization processes or capping agents. Furthermore, the nitrogen-mediated mechanism for the enhanced attachment of Ni nanoparticles is investigated through density functional theory (DFT) calculations.

In order to obtain CN_xMWNTs, a cobalt thin film on a SiO₂/Si substrate was deposited via rf sputtering as catalysts prior to the CN_xMWNTs growth step. CN_xMWNTs were then prepared by the catalytic decomposition of CH₄ and N₂ source gases via microwave plasma enhanced chemical vapor deposition. The nitrogen content in as-produced CN_xMWNTs analyzed by x-ray photoelectron spectroscopy ~3 at. %. Ni-CN_xMWNT hybrid materials were synthesized by reducing Ni precursor salt dissolved in ethylene glycol (EG) in the presence of NaOH as a reducing agent. 1 mL of 10 mM Ni (CH₃COO)₂·4H₂O EG solution and 8 mg of NaOH were mixed with 50 ml of EG in a vial. 5 mg of as-produced CN_xMWNTs was uniformly dispersed in the mixed solution by sonication. The vial was placed in the center of a household microwave oven and heated for 90 s. The black products were separated by centrifugation, washed with acetone, and dried. The obtained Ni-CN_xMWNTs were heat treated under the hydrogen atmosphere at 300 C in order to remove residual EG solution and reduce Ni oxide.

Figure 1 displays transmission electron microscopy (TEM) images of Ni-CN_xMWNT hybrid nanostructures. Figure 1(a) shows the TEM bright field image of typical Ni nanoparticles on CN_xMWNTs with a tube diameter ranging from 10 to 30 nm. Ni nanoparticles are uniformly dispersed on the sidewalls of the CN_xMWNTs, as clearly seen in the TEM dark field image [Fig. 1(b)]. The high-resolution TEM (HRTEM) image in Fig. 1(c) reveals that the CN_xMWNTs exhibit a bamboolike structure, the characteristic feature of nitrogen-containing CNTs. HRTEM images of this type were used to obtain the particle size distribution. The histogram of the diameters of Ni nanoparticles shows that they have a narrow size distribution ranging from 2 to 6 nm with a mean particle size of 3.5 nm as depicted in Fig. 1(e). Clear lattice fringes of the Ni nanoparticle firmly attached on the sidewall of the CN_xMWNTs are observed from the HRTEM image in Fig. 1(d). The EDX (Energy Dispersive X-ray) analysis

^{a)} Author to whom correspondence should be addressed; electronic mail: jeungku@kaist.ac.kr

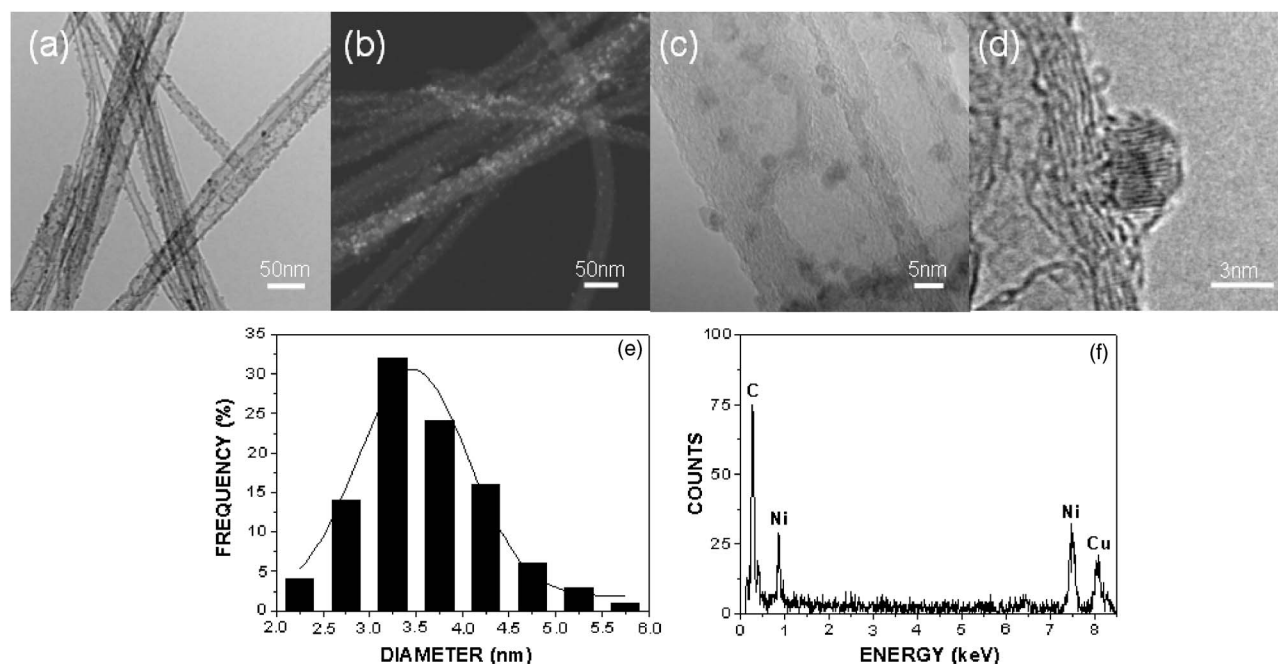


FIG. 1. (a) TEM bright field image of Ni nanoparticles on the sidewalls of CN_x MWNTs, (b) TEM dark field image of Ni nanoparticles on the sidewalls of CN_x MWNTs, (c) HRTEM image of Ni nanoparticles on the sidewalls of CN_x MWNTs, (d) HRTEM image of a single Ni nanoparticle on the sidewall of a CN_x MWNT, (e) a size histogram of Ni nanoparticles, and (f) EDX spectrum of the Ni nanoparticle shown in (d). The Cu peak arises from the TEM grid.

[Fig. 1(f)] confirms that the nanoparticle is a nickel cluster, not nickel oxide. It is noteworthy that uniformly dispersed metal nanoparticles with a narrow size distribution on CNTs can be established by a single chemical route through nitrogen mediation without functionalization processes or capping reagents. Control of the distribution and clustering of the metal nanoparticles arises from the binding energy of the metal with CNTs, considering that weak binding allows for fast surface diffusion. Therefore, the origin of the enhanced chemical reactivity can be understood in terms of the Ni binding energy with nitrogen doped CNTs.

The bonding configuration of nitrogen within CNTs has been investigated through experimental and theoretical approaches, leading to the identification of primarily two types of nitrogen configurations: pyridinelike where the nitrogen atom is bonded with two carbon atoms and graphitelike where the nitrogen atom replaces a graphitic carbon atom.^{23–26} Compound structures, vacancy-nitrogen complexes containing pyridinelike nitrogen atoms neighboring a carbon vacancy, have also been examined.^{25,26} Utilizing nitrogen-containing tube models, we also theoretically investigated the origin of the enhanced chemical reactivity obtained by the nitrogen mediation. Figure 2 displays the considered tube models containing (a) no nitrogen, (b) graphitelike nitrogen, (c) pyridinelike nitrogen, and (d) a vacancy-nitrogen complex in 11-layered (5,5) armchair tubes. All of the present calculations were performed using density functional theory (DFT), employing the B3LYP (Ref. 27) method. The basis set used in the calculation was 6-31G for carbon and hydrogen. 6-311+G** was used for nickel to describe the atomic orbitals of the Ni atom more accurately. The Ni binding energy is obtained from the expression $E_b = E[\text{Ni} + \text{tube}] - E[\text{tube}] - E[\text{Ni}]$, where $E[\text{Ni} + \text{tube}]$ is the total energy of the Ni adsorbed on the doped or undoped tube, $E[\text{tube}]$ is the total energy of the doped or undoped tube, and $E[\text{Ni}]$ is the total energy of the isolated Ni atom.

For comparison, the Ni binding energy on the sidewall of the undoped tube was initially calculated as a reference, reflecting that most energetic binding of the Ni atom occurs at the bridge site (over a C–C bond tilted to tube axis), as determined by the authors in a previous investigation.²⁸ The Ni binding energy calculated for the undoped tube is -0.47 eV [Fig. 3(a)]. The Ni binding for the nitrogen-containing tubes was then assessed. First, for the tube containing graphitelike nitrogen, optimized structures and corresponding binding energies are shown in Fig. 3(b)–3(d). Contrary to expectations, the Ni atom directly bound to the graphitelike nitrogen [Fig. 3(b)] shows weaker binding energy (-0.34 eV) than the undoped tube. Interestingly, the graphitelike nitrogen enhances the Ni binding energy by means of chemically activating surrounding carbon atoms in the tube, showing that the Ni atom binds more favorably to the C–C bond neighboring nitrogen atom, as depicted in Figs. 3(c) and 3(d), with Ni binding energies of -0.68 and

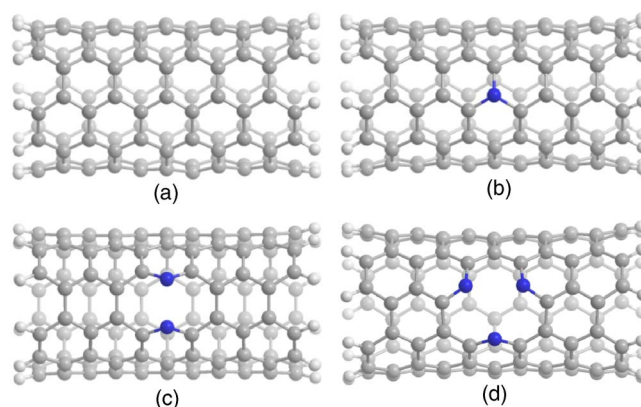


FIG. 2. (Color online) Considered tube structures containing (a) no nitrogen, (b) graphitelike nitrogen, (c) pyridinelike nitrogen where two nitrogen atoms neighbor each other, and (d) a vacancy-nitrogen complex consisting of three pyridinelike nitrogen atoms neighboring a carbon vacancy.

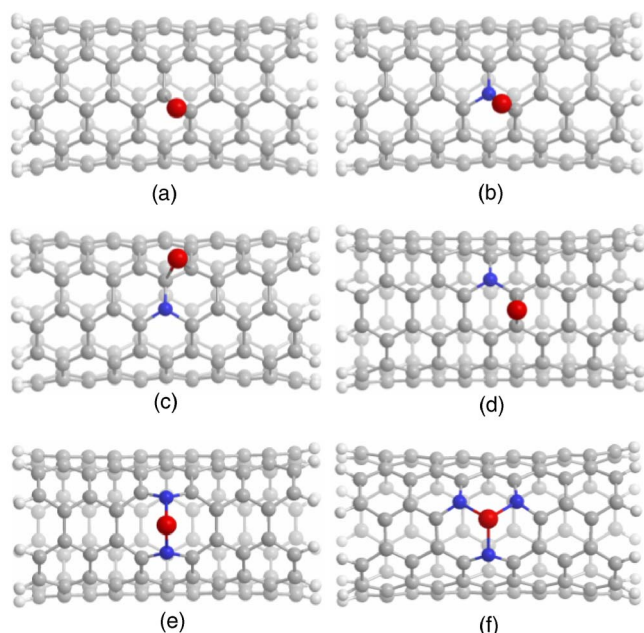


FIG. 3. (Color online) Optimized structures of Ni bound to tubes containing (a) no nitrogen, [(b)–(d)] graphitelike nitrogen, (e) pyridinelike nitrogen, and (f) a vacancy-nitrogen complex. The calculated Ni binding energies are (a) -0.47 eV, (b) -0.34 eV, (c) -0.68 eV, (d) -0.66 eV, (e) -1.62 eV, and (f) -4.59 eV. The graphitelike nitrogen contributes to the enhancement of the Ni binding energy by activating surrounding carbon atoms whereas pyridinelike nitrogen strongly binds to the Ni atom as shown in (e) and (f).

-0.66 eV, respectively. Compared to the graphitelike nitrogen, the pyridinelike nitrogen significantly strengthens Ni adsorption. Figures 3(e) and 3(f) show the optimized structures of the Ni atom bound to the pyridinelike nitrogen atoms, revealing binding energies of -1.62 and -4.59 eV, respectively. This indicates that the binding energy of metals can be significantly increased by the introduction of nitrogen, the so-called nitrogen-mediated mechanism. It is also observed that, contrary to the graphitelike nitrogen, pyridinelike nitrogen can directly contribute to the enhancement of the Ni binding energy, reflecting that the Ni atom strongly binds to the pyridinelike nitrogen atoms. This different behavior is attributed to the molecular orbital associated with different configurations of nitrogen in sp^2 carbon networks: the graphitelike nitrogen uses three valence electrons for sigma bonds, one for the π bond, and the remaining one to generate a π^* state that can activate neighboring carbon atoms. In contrast, the pyridinelike nitrogen uses two valence electrons for sigma bonds, one for the π bond, and the remaining two to form a filled p -like nonbonding state. This p -like nonbonding of the pyridine-like nitrogen results in the strong hybridization with the d orbital of the Ni atom, as visualized in the molecular orbital diagrams (Fig. S3).

In summary, we have shown that Ni-carbon-nanotube hybrid materials can be established by a single chemical route through nitrogen mediation without functionalization processes or capping reagents. Ni nanoparticles were uniformly dispersed and had a narrow size distribution ranging from 2 to 6 nm with a mean particle size of 3.5 nm. The origin of the enhanced chemical reactivity, the so-called nitrogen-mediated mechanism, has been explained in terms of the Ni binding energy with nitrogen doped CNTs through DFT calculations. Graphitelike nitrogen contributes to enhanced Ni binding energy by means of activating neighbor-

ing carbon atoms, whereas pyridinelike nitrogen strongly binds to the Ni atom. The pyridine-like nitrogen atoms neighboring a carbon vacancy showed strongest interaction with the Ni atom, relative to that for the undoped tube. Clearly, it is possible to control the clustering of metals by increasing the binding energy of metals via the introduction of nitrogen, an important issue in fabricating transition metal-carbon nanotube hybrid materials. Meanwhile, further study to elucidate the effect of nitrogen atoms on hydrogen storage capacity of Ni-CN_xMWNTs would be interesting, considering that Ni nanoparticles on MWNTs enhance the hydrogen storage capacity.⁴

This work was supported by Grant No. R01-2005-000-10333-0 from the Basic Research Program of the Korea Science and Engineering Foundation and the Korea Research Foundation Grant funded by the Korean Government (MOEHRD) (KRF-2005-005-J09703).

¹T. Yildirim and S. Ciraci, Phys. Rev. Lett. **94**, 175501 (2005).

²J. Kong, M. G. Chapline, and H. Dai, Adv. Mater. (Weinheim, Ger.) **13**, 1384 (2001).

³Q. Zhao, M. B. Nardelli, W. Lu, and J. Bernholc, Nano Lett. **5**, 847 (2005).

⁴H. S. Kim, H. Lee, K. S. Han, J. H. Kim, M. S. Song, M. S. Park, J. Y. Lee, and J. K. Kang, J. Phys. Chem. B **109**, 8983 (2005).

⁵E. Durgun, S. Dag, V. M. K. Bagci, O. Gulseren, T. Yildirim, and S. Ciraci, Phys. Rev. B **67**, 201401 (2003).

⁶W. Li, C. Liang, W. Zhou, J. Qiu, Z. H. Zhou, G. Sun, and Q. Xin, J. Phys. Chem. B **107**, 6292 (2003).

⁷A. Javey, R. Tu, D. B. Farmer, J. Guo, R. G. Gordon, and H. Dai, Nano Lett. **5**, 345 (2005).

⁸G. G. Wildgoose, C. E. Banks, and R. G. Compton, Small **2**, 182 (2006).

⁹R. H. Bauhman, A. A. Zakhidov, and W. A. de Heer, Science **297**, 787 (2002).

¹⁰G. Che, B. B. Lakshmi, E. R. Fisher, and C. R. Martin, Nature (London) **393**, 346 (1998).

¹¹H. Zhang, J. Qiu, C. Liang, Z. Li, X. Wang, Y. Wang, Z. Feng, and C. Li, Catal. Lett. **101**, 211 (2005).

¹²J.-P. Tessonier, L. Pesant, G. Ehret, M. J. Ledoux, and C. Pham-Huu, Appl. Catal., A **142**, 169 (2005).

¹³S. F. Yin, B. Q. Xu, W. X. Zhu, C. F. Ng, X. P. Zhou, and C. T. Au, Catal. Today **93–95**, 27 (2004).

¹⁴H. Hu, B. Zhao, M. A. Hamon, K. Kamaras, M. E. Itkis, and R. C. Haddon, J. Am. Chem. Soc. **125**, 14893 (2003).

¹⁵J. Zhang, H. Zou, Q. Qing, Y. Yang, Q. Li, Z. Liu, X. Guo, and Z. Du, J. Phys. Chem. B **107**, 3712 (2003).

¹⁶S. Banerjee, T. Hemraj-Benny, and S. S. Wong, Adv. Mater. (Weinheim, Ger.) **17**, 17 (2005).

¹⁷C. A. Dyke and J. M. Tour, J. Phys. Chem. A **108**, 11151 (2004).

¹⁸K. S. Coleman, S. R. Bailey, S. Fogden, and M. L. H. Green, J. Am. Chem. Soc. **125**, 8722 (2003).

¹⁹J. L. Hudson, M. J. Casavant, and J. M. Tour, J. Am. Chem. Soc. **126**, 11158 (2004).

²⁰R. Czerw, M. Terrones, J. -C. Charlier, X. Blase, B. Foley, R. Kamalakaran, N. Grobert, H. Terrones, D. Tekleab, P. M. Ajayan, W. Blau, M. Ruhle, and D. L. Carroll, Nano Lett. **1**, 457 (2001).

²¹S. Peng and K. Cho, Nano Lett. **3**, 513 (2003).

²²A. H. Nevidomskyy, G. Csanyi, and M. C. Payne, Phys. Rev. Lett. **91**, 105502 (2003).

²³H. C. Choi, J. Park, and B. Kim, J. Phys. Chem. B **109**, 4333 (2005).

²⁴L. H. Chan, K. H. Hong, D. Q. Xiao, T. C. Lin, S. H. Lai, W. J. Hsieh, and H. C. Shih, Phys. Rev. B **70**, 125408 (2004).

²⁵H. S. Kang and S. Jeong, Phys. Rev. B **70**, 233411 (2004).

²⁶A. G. Kudashov, A. V. Okotrub, L. G. Bulusheva, I. P. Asanov, Y. V. Shubin, N. F. Yudanov, L. I. Yudanov, V. S. Danilovich, and O. G. Abrosimov, J. Phys. Chem. B **108**, 9048 (2004).

²⁷A. D. Becke, J. Chem. Phys. **98**, 5648 (1993).

²⁸S. H. Yang, W. H. Shin, J. W. Lee, S. Y. Kim, S. I. Woo, and J. K. Kang, J. Phys. Chem. B **110**, 13941 (2006).